

# Stability of trions in coupled quantum wells modelled by two-dimensional bilayers

O. Witham,<sup>1,2</sup> R. J. Hunt,<sup>2</sup> and N. D. Drummond<sup>2</sup>

<sup>1</sup>*Institut für Theoretische Physik, Goethe-Universität Frankfurt, 60438 Frankfurt am Main, Germany*

<sup>2</sup>*Department of Physics, Lancaster University, Lancaster LA1 4YB, United Kingdom*

(Dated: August 31, 2022)

We report variational and diffusion quantum Monte Carlo calculations of the binding energies of indirect trions and biexcitons in ideal two-dimensional bilayer systems within the effective-mass approximation, and with a Coulomb  $1/r$  interaction between charge carriers. The critical layer separation at which trions become unbound has been studied for various electron-hole mass ratios, and found to be over an order of magnitude larger than the critical layer separation for biexcitons. Trion formation may significantly inhibit the formation of Bose-Einstein condensates of indirect excitons in coupled quantum-well bilayer systems.

PACS numbers: 71.35.Cc, 71.35.Pq, 78.67.De, 02.70.Ss, 67.85.Hj, 67.85.Jk

## I. INTRODUCTION

Excitonic complexes consisting of bound states of small numbers of electrons and holes have been observed under many different conditions in semiconductors. In the dilute limit, excitons collectively behave as a gas of weakly interacting neutral bosons. It was first predicted in the 1960s that Bose-Einstein condensates (BECs) of excitons might form under experimentally accessible conditions,<sup>1</sup> and coupled quantum-well heterostructures, in which electrons and holes are confined to spatially separated layers, were later identified as an ideal testbed for the observation of an excitonic BEC.<sup>2</sup> Such geometries hinder recombination and significantly increase the exciton lifetime, which is necessary if thermalization of a photoexcited gas of excitons is to occur. Furthermore, at sufficiently large layer separations, the repulsive dipole-dipole interaction between spatially indirect excitons helps to prevent the formation of larger charge-carrier complexes. However, despite extensive searches, studies claiming direct observation of an excitonic BEC have so far led to inconclusive results.<sup>3–6</sup> The formation of biexcitons (also neutral composite bosons, but with a higher mass than excitons) could potentially inhibit condensation, but various theoretical works<sup>7–10</sup> showed that biexcitons are expected to be unbound in the typical coupled quantum-well geometries accessible to experimentalists, in which the layer separation is of the order of tens of Ångströms.

Although biexcitons in coupled quantum wells have been studied extensively, to our knowledge there have been no previous theoretical studies of indirect trions (charged excitons) in coupled quantum wells. Trion formation can occur if a nonzero concentration of free charge carriers is present in a sample; these charge carriers then bind to the excitons created by optical excitation. Trions are composite fermions and hence the formation of trions would inhibit BEC. Furthermore, it is known that trions play a key role in the optical properties of atomically thin transition-metal dichalcogenides and other two-dimensional (2D) semiconductors.<sup>11–16</sup> In this work we study spatially indirect trions in bilayer sys-

tems. We shall assume an isotropically screened Coulomb interaction, as appropriate for trions in GaAs/AlGaAs heterostructures, rather than the Keldysh interaction appropriate for charge carriers in 2D systems with a significant in-plane polarizability.<sup>17,18</sup> Nevertheless, our results are of qualitative relevance to studies of bilayers of 2D semiconductors.

We have used the variational and diffusion quantum Monte Carlo (VMC and DMC) methods<sup>19,20</sup> to calculate the ground-state energies and binding energies of spatially indirect trions within the 2D-isotropic effective-mass approximation. A negative trion in such an ideal 2D bilayer system is approximately described by the Hamiltonian

$$\hat{H} = -\frac{\hbar^2}{2m_e}\nabla_{\mathbf{e}_1}^2 - \frac{\hbar^2}{2m_e}\nabla_{\mathbf{e}_2}^2 - \frac{\hbar^2}{2m_h}\nabla_{\mathbf{h}}^2 + \frac{e^2}{4\pi\epsilon r_{ee}} - \frac{e^2}{4\pi\epsilon\sqrt{r_{e_1h}^2 + d^2}} - \frac{e^2}{4\pi\epsilon\sqrt{r_{e_2h}^2 + d^2}}, \quad (1)$$

where  $m_e$  and  $m_h$  are the electron and hole effective masses,  $e$  is the magnitude of electronic charge,  $d$  is the interlayer separation, and  $\epsilon$  is the permittivity of the medium in which the two layers are embedded. The in-plane interparticle distances are given by  $r_{ee} = |\mathbf{r}_{e_1} - \mathbf{r}_{e_2}|$  and  $r_{e_ih} = |\mathbf{r}_{e_i} - \mathbf{r}_h|$ , where  $\mathbf{r}_{e_1}$ ,  $\mathbf{r}_{e_2}$ , and  $\mathbf{r}_h$  are 2D vectors holding the in-plane coordinates of the electrons and the hole, which are assumed to be confined to parallel planes as shown in Fig. 1. Although our results pertain directly to the negative trion ( $X^-$ ), the corresponding properties of the positive trion ( $X^+$ ) can easily be generated by charge conjugation, i.e., by interchanging  $m_e$  and  $m_h$  (or, equivalently, by replacing  $\sigma$  by  $\sigma^{-1}$ ). Furthermore, we consider only the ground-state case in which the two electrons are distinguishable (opposite-spin electrons). Trions and biexcitons with indistinguishable electrons are much less stable than trions with distinguishable electrons; by analogy with results obtained for biexcitons in single-layer 2D semiconductors, we expect that trions and biexcitons with indistinguishable particles are only stable when the indistinguishable particles are very heavy, so that exchange effects are negligible.<sup>18</sup>

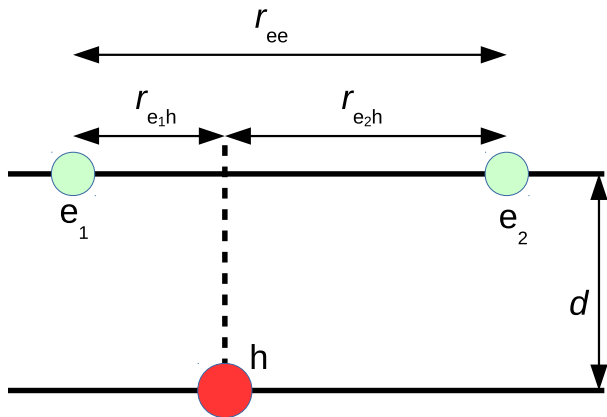


FIG. 1. (Color online) Schematic arrangement of two electrons (light green) and a hole (red) for a negative trion in a coupled quantum well, showing the definition of the interparticle distances. The two electrons are in a spin singlet state and hence act as distinguishable particles in the spatial wave function. The electrons and hole move in 2D in spatially separated layers.

The rest of this paper proceeds as follows. In Sec. II we describe our methodology for calculating the binding energies of trions and biexcitons; in Sec. III we present our results; and finally in Sec. IV we draw our conclusions. Except where otherwise stated, we use excitonic units: energies are given in terms of the exciton Rydberg  $R_y^* = \mu e^4 / [2(4\pi\epsilon\hbar)^2]$  and lengths are given in terms of the exciton Bohr radius  $a_0^* = 4\pi\epsilon\hbar^2 / (\mu e^2)$ , where  $\mu = m_e m_h / (m_e + m_h)$  is the reduced mass of the electron and hole. In these units the dimensionless solutions  $E/R_y^*$  to the Schrödinger equation only depend on the electron-hole mass ratio  $\sigma = m_e/m_h$  and the dimensionless layer separation  $d/a_0^*$ .

## II. COMPUTATIONAL METHODOLOGY

The VMC and DMC methods<sup>19,20</sup> as implemented in the CASINO code<sup>21</sup> were used in conjunction with a trial wave function of the form

$$\Psi = \exp(J)\Psi_{ee}\Psi_{e_1h}\Psi_{e_2h}, \quad (2)$$

where

$$\Psi_{ee} = \exp\left[\frac{c_1 r_{ee}}{1 + c_2 r_{ee}} + \frac{1}{2} \left(e^{-c_6 r_{ee}^2} - 1\right) \log(r_{ee})\right] \quad (3)$$

$$\Psi_{e_1h} = \exp\left[\frac{c_3 r_{e_1h} + c_4 r_{e_1h}^2}{1 + c_5 r_{e_1h}}\right] \quad (4)$$

$$\Psi_{e_2h} = \exp\left[\frac{c_3 r_{e_2h} + c_4 r_{e_2h}^2}{1 + c_5 r_{e_2h}}\right], \quad (5)$$

to perform total-energy calculations for the negative trion. Our trial wave function is similar to the one used

by Tan *et al.* to study biexcitons,<sup>22</sup> but with an additional term that describes the behavior of the wave function when one electron is far from the remaining exciton. The nested exponential in Eq. (3) acts as a “switching on” term; the logarithm only manifests appreciably in the case that the two electrons are far apart. The Jastrow exponent  $J$  contains cusplike two-body and three-body polynomial functions of the interparticle distances, truncated at finite range.<sup>23,24</sup> The wave function of Eqs. (2)–(5) incorporates both short- and long-range effects through the use of the Padé-form exponents. It exhibits the correct symmetry of the ground-state system, being invariant upon the exchange of the two electrons, i.e.,  $\Psi(\mathbf{r}_{e_1}, \mathbf{r}_{e_2}, \mathbf{r}_h) = \Psi(\mathbf{r}_{e_2}, \mathbf{r}_{e_1}, \mathbf{r}_h)$ . The trial wave function reduces to

$$\Psi \rightarrow A \frac{1}{\sqrt{r_{ee}}} \exp[-k r_{ee}] \exp\left[\frac{c_3 r_{e_2h} + c_4 r_{e_2h}^2}{1 + c_5 r_{e_2h}}\right], \quad (6)$$

when one electron is far from the remaining exciton, where  $k > 0$  and  $A$  is constant. This form of wave function is appropriate for an electron moving in the potential energy due to the static charge distribution of the remaining indirect exciton. The static dipole moment of an exciton is  $\mathbf{p} = -ed\mathbf{e}_z$ , where  $\mathbf{e}_z$  is a unit vector in the  $z$  direction. Let the separation of the electron from the center of the exciton be  $\mathbf{r} + (d/2)\mathbf{e}_z$ , where  $\mathbf{r}$  is the in-plane separation. Hence the long-range exciton-electron interaction energy is

$$-e\mathbf{p} \cdot [\mathbf{r} + (d/2)\mathbf{e}_z] / [4\pi\epsilon|\mathbf{r} + (d/2)\mathbf{e}_z|^3] \sim r^{-3}. \quad (7)$$

Solving the 2D radial Schrödinger equation for motion in a rapidly decaying potential such as  $r^{-3}$  gives the form of wave function shown in Eq. (6) at long range.

The parameter set  $\{c_1, \dots, c_6\}$  is subject to the following conditions: (i) The values of  $c_1$  and  $c_3$  are fixed by the electron-electron and electron-hole Kato cusp conditions;<sup>25,26</sup> (ii)  $c_4 < 0$  to ensure that the wave function falls off exponentially as  $r_{e_ih} \rightarrow \infty$ ; (iii)  $c_2, c_5 > 0$  to avoid divergences in the wave function; and (iv)  $c_6 > 0$  to enforce the correct long-range behavior of an electron in a dipole field. The optimal values of the parameters  $\{c_1, \dots, c_6\}$  were obtained by successive minimization of the variance of the local energy and the energy expectation value.<sup>27–29</sup>

In the DMC method the ground-state component of the trial wave function is projected out by simulating a stochastic process governed by the Schrödinger equation in imaginary time. In systems such as those considered here, in which there are no indistinguishable fermions, there are no uncontrolled approximations in the DMC ground-state energy. We simultaneously remove time-step bias and population-control bias by performing DMC calculations at two different, small time steps, with the walker population being in inverse proportion to the time step, and extrapolating linearly to zero time step.

The binding energy  $E_{X^-}^b$  of a negative trion is defined as the energy required to split the trion into an exciton and a free electron, i.e.,

$$E_{X^-}^b = E_X - E_{X^-}, \quad (8)$$

where  $E_X$  and  $E_{X^-}$  are the ground-state total energies of an exciton and a negative trion, respectively. Instability of the trion with respect to dissociation into a free electron and an indirect exciton is signalled by difficulty optimizing a bound-state trial wave function, followed by the occurrence of nonpositive  $E_{X^-}^b$  values in DMC calculations in which the trial wave function is forced to be bound. The curve defined by  $E_{X^-}^b(d/a_0^*, \sigma) = 0$ , where  $E_{X^-}^b(d/a_0^*, \sigma)$  is the binding energy of the trion with a given electron-hole mass ratio  $\sigma$  and dimensionless layer separation  $d/a_0^*$ , defines the boundary of the stability region of the trion. In practice we invert this relation and simply quote the critical layer separation  $d_{X^-}^{\text{crit}}(\sigma)$  as a function of mass ratio. We have attempted to probe the trion stability region directly by studying systems with electron-hole mass ratios  $\sigma = 1/4, 1/2, 3/4, 1, 4/3, 2$ , and 4, and fitting the resultant trion binding energies to a Padé approximant of the form

$$\frac{E_{X^-}^b(d/a_0^*)}{R_y^*} = \frac{E_{X^-}^b(0)/R_y^* + \sum_{i=1}^3 a_i (d/a_0^*)^i}{1 + \sum_{j=1}^4 b_j (d/a_0^*)^j}, \quad (9)$$

where  $\{a_i\}$  and  $\{b_j\}$  are fitting parameters. We have found that this functional form yields sufficiently accurate fits of the binding energies for all mass ratios considered here.

Where the trion is bound, we have performed fits to a ‘‘partial 2D’’ Padé approximant of the form

$$\frac{E_{X^-}^b(\sigma, d/a_0^*)}{R_y^*} = \frac{\sum_{i=0}^3 \sum_{j=0}^3 f_{ij} (1 + \sigma)^{-i/2} (d/a_0^*)^j}{1 + \sum_{k=1}^4 g_k (d/a_0^*)^k}, \quad (10)$$

where  $f_{ij}$  and  $g_k$  are fitting parameters, and the  $\sigma$  dependence is motivated by the harmonic approximation within the Born-Oppenheimer approximation in the case that  $\sigma \rightarrow \infty$ .<sup>18,30</sup>

Finally, we report pair-distribution functions (PDFs), which give information about the structure and spatial extent of charge-carrier complexes. For a negative trion, the electron-electron and electron-hole PDFs are defined via

$$g_{X^-}^{\text{ee}}(\mathbf{r}) = \langle \delta(\mathbf{r} - \mathbf{r}_{\text{ee}}) \rangle \quad (11)$$

$$g_{X^-}^{\text{eh}}(\mathbf{r}) = \left\langle \sum_{i=1}^2 \delta(\mathbf{r} - \mathbf{r}_{\text{e},i\text{h}}) \right\rangle. \quad (12)$$

The PDFs in a biexciton are defined in an analogous fashion. The PDFs are evaluated by binning the interparticle distances sampled in the VMC and DMC calculations. The error in the VMC and DMC estimates of the PDF is first order in the error in the trial wave function; however, the error in the extrapolated estimate

of the PDF, given by two times the DMC result minus the VMC result, is second order in the error in the trial wave function.<sup>31</sup> The PDF results that we report were obtained by extrapolated estimation.

### III. RESULTS AND DISCUSSION

#### A. Trion binding energy and region of stability

Our negative-trion binding-energy results are displayed in Fig. 2, and our predicted critical layer separations are shown in Table I. For larger electron-hole mass ratios  $\sigma$ , the binding energy decays slowly to zero, and furthermore the DMC calculations become more difficult due to the separation of imaginary-time scales for the different particles. The inset to Fig. 2 illustrates the challenge in determining a precise value for the boundary of the region of stability. Nevertheless, we can easily place lower bounds on the critical layer separation at a given mass ratio. As can be seen in Fig. 2 and Table I, trions are stable over a large region of the  $(d/a_0^*, \sigma)$  model parameter space. When compared with the biexciton stability region,<sup>10</sup> we find that the trion is bound for layer separations over an order of magnitude larger than those for which the biexciton is bound. Trion formation is always possible whenever biexcitons are bound, and trion binding energies are typically far larger for the same set of material parameters.

TABLE I. Critical layer separations for negative trions ( $d_{X^-}^{\text{crit}}$ ) and biexcitons ( $d_{XX}^{\text{crit}}$ ) at different electron-hole mass ratios  $\sigma$ . The biexciton critical layer separations were evaluated using Eq. (2) of Ref. 10.

$\sigma$	$d_{X^-}^{\text{crit}}/a_0^*$	$d_{XX}^{\text{crit}}/a_0^*$ (Ref. 10)
1/4	4.52(4)	0.48
1/2	5.26(6)	0.43
3/4	6.63(9)	0.42
1	7.69(7)	0.42
4/3	> 8	0.42
2	> 8	0.43
4	> 8	0.48

The biexciton (XX), whose dominant decay is into a pair of excitons ( $XX \rightarrow X+X$ ), has a stability region that is determined by the effective interactions of the constituent indirect excitons, and this effective interaction is a repulsive dipole-dipole interaction at long range.<sup>8,10</sup> Negative-trion dissociation is determined by the effective interaction of a lone electron with a single indirect exciton. The interaction potential between an indirect exciton and a lone electron consists of a repulsive part due to the static charge distribution of the exciton, which falls off as  $r^{-3}$ , and an attractive part due to the induced

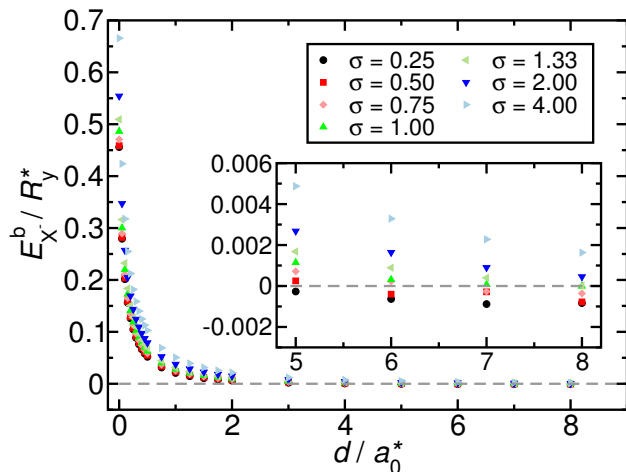


FIG. 2. (Color online) Negative-trion binding energy as a function of interlayer spacing  $d$  and electron-hole mass ratio  $\sigma$ , in excitonic units. The inset shows the edge of the region of stability for negative trions in greater detail.

dipole moment of the exciton, which falls off as  $r^{-4}$ . Over the intermediate range the attractive part of the interaction plays a much more important role in the trion than in the biexciton.

Fitting Eq. (10) to our trion binding energies results in a maximum error of  $5 \times 10^{-4} R_y^*$ , with over 90% of the data points falling within  $2 \times 10^{-4} R_y^*$  of the fit. The fitting parameters  $f_{ij}$  and  $g_k$  are<sup>32</sup>

$$f = \begin{pmatrix} 1.408 & 21.53 & 25.25 & 1.676 \\ -2.340 & -40.43 & -36.22 & -11.51 \\ 1.617 & 30.47 & 5.803 & 17.36 \\ -0.2129 & -0.5492 & 7.423 & -8.694 \end{pmatrix} \quad (13)$$

$$g = \begin{pmatrix} 26.16 \\ 147.7 \\ 186.4 \\ 29.45 \end{pmatrix}. \quad (14)$$

This fit applies only for  $1/4 \leq \sigma \leq 4$  and  $0 \leq d \leq \min\{8a_0^*, d_{X^-}^{\text{crit}}\}$ . Accurately parameterizing the binding energy near the critical separation  $d_{X^-}^{\text{crit}}$  is not possible with our limited data, and caution should be applied when relying on this fit near the critical region.

Appropriate model parameters for the GaAs/AlGaAs coupled quantum-well device studied by Butov *et al.*<sup>3</sup> were identified in Ref. 22. The electron and hole masses are taken to be  $m_e = 0.067m_0$  and  $m_h = 0.134m_0$ , where  $m_0$  is the bare electron mass. The permittivity is taken to be  $\epsilon = 13.2\epsilon_0$ . Hence the mass ratio is  $\sigma = 0.5$ , the exciton Bohr radius is  $a_0^* = 156 \text{ \AA}$ , and the exciton Rydberg is  $R_y^* = 3.5 \text{ meV}$ . Finally, the layer separation is taken to be  $d = 100 \text{ \AA} = 0.64a_0^*$ .

With these parameters, Lee *et al.*<sup>10</sup> found the critical layer separation for biexciton formation to be  $d_{XX}^{\text{crit}}(0.5) =$

$0.43(5)a_0^* = 67(8) \text{ \AA}$ . This is significantly less than the actual layer separation, implying that biexcitons are unbound. On the other hand, we find the critical layer separation for negative-trion formation to be  $d_{X^-}^{\text{crit}}(0.5) = 5.26(6)a_0^* = 821(9) \text{ \AA}$  and the critical layer separation for positive-trion formation to be  $d_{X^+}^{\text{crit}}(2) > 8a_0^* = 1248 \text{ \AA}$ . Both of these are many times larger than the actual layer separation, implying that both positive and negative trions are bound. Using Eq. (9), the predicted binding energies of negative and positive trions are  $0.0411(4)R_y^* = 0.14 \text{ meV}$  and  $0.06166(3)R_y^* = 0.22 \text{ meV}$ , respectively. Hence both positive and negative trions are expected to be present at temperatures below  $T = 2 \text{ K}$ , which corresponds to an energy of about  $k_B T = 0.17 \text{ meV}$ . We therefore believe that trion formation could have played a role in inhibiting the formation of a BEC in the experimental setup of Butov *et al.* The situation is not entirely clearcut, however, because the concentration of trions might be low due to the low concentration of pre-existing charge carriers at the time of optical excitation.

## B. Biexciton binding energy

In an extension to the earlier work of Lee *et al.*,<sup>10</sup> for completeness we provide an accurate parameterization of the biexciton binding energy in the bound region. We have used the same trial wave function form as in Ref. 22, multiplied by a polynomial Jastrow factor.<sup>23,24</sup> We have fitted the function

$$\frac{E_{XX}^b(\sigma, d/a_0^*)}{R_y^*} = \frac{\sum_{i=0}^2 \sum_{j=0}^2 F_{ij} (\sigma + \sigma^{-1})^{i/2} (d/a_0^*)^j}{\sum_{k=0}^3 G_k (d/a_0^*)^k} \quad (15)$$

to our biexciton binding-energy data, where  $F_{ij}$  and  $G_k$  are fitting parameters. This obeys the necessary symmetry under charge conjugation ( $\sigma \rightarrow \sigma^{-1}$ ). As in Eq. (10), the square-root behavior in Eq. (15) arises from harmonic motion in the Born-Oppenheimer approximation.<sup>18</sup> Our fit of Eq. (15) has a maximum error of  $2 \times 10^{-2} R_y^*$ , with over 90% of the data points falling within  $5 \times 10^{-3} R_y^*$  of the fit. The results of this fit are

$$F = \begin{pmatrix} 0.03495 & -0.9822 & 2.437 \\ 0.07670 & 0.3303 & -1.786 \\ -0.005277 & -0.02931 & 0.2942 \end{pmatrix} \quad (16)$$

$$G = \begin{pmatrix} 0.1726 \\ 3.256 \\ 1.567 \\ 29.95 \end{pmatrix}. \quad (17)$$

## C. PDFs

In Fig. 3 we plot electron-electron and electron-hole pair-distribution functions for negative trions. It is clear

that the spatial extent of the trion increases rapidly with layer separation, but is relatively insensitive to mass ratio.

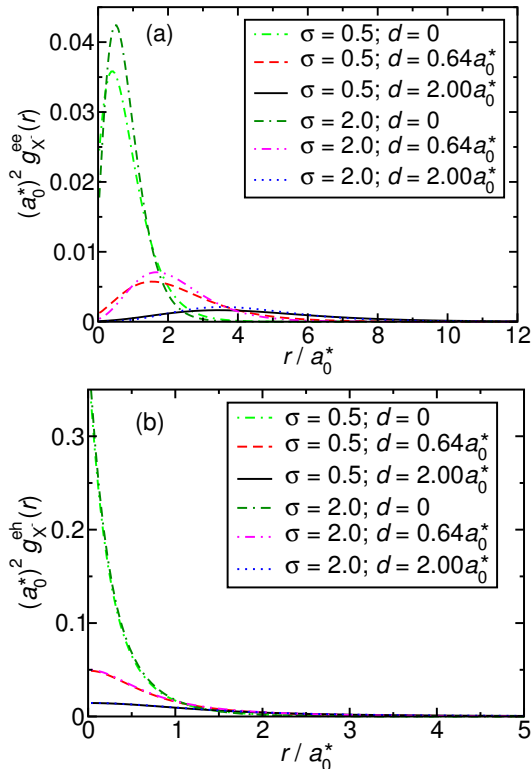


FIG. 3. (Color online) (a) Electron-electron [ $g_{X-}^{ee}(r)$ ] and (b) electron-hole [ $g_{X-}^{eh}(r)$ ] pair-distribution functions for indirect negative trions in bilayers with different separations  $d$  and electron-hole mass ratios  $\sigma$ . The  $x$ -axis shows the in-plane separation.

## IV. CONCLUSIONS

We have generated statistically exact total-energy data for indirect trions and biexcitons in a simple model of charge-carrier complexes in coupled quantum-well heterostructures. We have found that for indirect trions, the critical layer separation at which the trion becomes unbound is at least an order of magnitude larger than that of the biexciton.

We have applied our results to the coupled quantum-well device studied by Butov *et al.*,<sup>3</sup> as modelled by Tan *et al.*<sup>22</sup> We find that, although biexcitons are unbound in this system, positive and negative trions are bound, with substantial binding energies. The formation of trions, which are composite fermions, could therefore hinder the formation of a BEC of excitons. Qualitatively similar physics is expected in bilayers of 2D materials, where the interlayer and intralayer charge-charge interactions reduce to the Coulomb  $1/r$  form studied here at long range. In 2D materials the binding energy of the trion relative to the biexciton is further magnified by the nonlocal screening of the charge carriers by the 2D layers.<sup>16</sup>

## ACKNOWLEDGMENTS

Computational resources were provided by Lancaster University's High-End Computing facility. R. J. H. is fully funded by the Graphene NOWNANO centre for doctoral training (grant no. EP/L01548X/1). We acknowledge useful conversations with R. J. Needs and M. Szyniszewski.

<sup>1</sup> J. M. Blatt, K. W. Böer, and W. Brandt, Phys. Rev. **126**, 1691 (1962).  
<sup>2</sup> X. Zhu, P. B. Littlewood, M. S. Hybertsen, and T. M. Rice, Phys. Rev. Lett. **74**, 1633 (1995).  
<sup>3</sup> L. V. Butov, A. C. Gossard, and D. S. Chemla, Nature **418**, 751 (2002).  
<sup>4</sup> D. Snoke, S. Denev, Y. Liu, L. Pfeiffer, and K. West, Nature **418**, 754 (2002).  
<sup>5</sup> L. V. Butov, L. S. Levitov, A. V. Mintsev, B. D. Simons, A. C. Gossard, and D. S. Chemla, Phys. Rev. Lett. **92**, 117404 (2004).  
<sup>6</sup> R. Rapaport, G. Chen, D. Snoke, S. H. Simon, L. Pfeiffer, K. West, Y. Liu, and S. Denev, Phys. Rev. Lett. **92**, 117405 (2004).  
<sup>7</sup> R. Zimmermann and C. Schindler, Solid State Commun. **144**, 395 (2007).  
<sup>8</sup> C. Schindler and R. Zimmermann, Phys. Rev. B **78**, 045313 (2008).  
<sup>9</sup> A. D. Meyertholen and M. M. Fogler, Phys. Rev. B **78**, 235307 (2008).

<sup>10</sup> R. M. Lee, N. D. Drummond, and R. J. Needs, Phys. Rev. B **79**, 125308 (2009).  
<sup>11</sup> K. F. Mak, K. He, C. Lee, G. H. Lee, J. Hone, T. F. Heinz, and J. Shan, Nat. Mater. **12**, 207 (2013).  
<sup>12</sup> C. Zhang, H. Wang, W. Chan, C. Manolatou, and F. Rana, Phys. Rev. B **89**, 205436 (2014).  
<sup>13</sup> A. Srivastava, M. Sidler, A. V. Allain, D. S. Lembke, A. Kis, and A. Imamoglu, Nat. Phys. **11**, 141 (2015).  
<sup>14</sup> D. K. Zhang, D. W. Kidd, and K. Varga, Nano Letters **15**, 7002 (2015).  
<sup>15</sup> A. M. Jones, H. Yu, N. J. Ghimire, S. Wu, G. Aivazian, J. S. Ross, B. Zhao, J. Yan, D. G. Mandrus, D. Xiao, W. Yao, and X. Xu, Nat. Nanotechnol. **8**, 634 (2013).  
<sup>16</sup> M. Szyniszewski, E. Mostaani, N. D. Drummond, and V. I. Fal'ko, Phys. Rev. B **95**, 081301 (2017).  
<sup>17</sup> L. V. Keldysh, JETP **29**, 658 (1979).  
<sup>18</sup> E. Mostaani, M. Szyniszewski, C. H. Price, R. Maezono, M. Danovich, R. J. Hunt, N. D. Drummond, and V. I. Fal'ko, ArXiv e-prints (2017), arXiv:1706.04688 [cond-mat.mes-hall].

- <sup>19</sup> D. M. Ceperley and B. J. Alder, Phys. Rev. Lett. **45**, 566 (1980).
- <sup>20</sup> W. M. C. Foulkes, L. Mitas, R. J. Needs, and G. Rajagopal, Rev. Mod. Phys. **73**, 33 (2001).
- <sup>21</sup> R. J. Needs, M. D. Towler, N. D. Drummond, and P. López Ríos, J. Phys. Condens. Matter **22**, 023201 (2010).
- <sup>22</sup> M. Y. J. Tan, N. D. Drummond, and R. J. Needs, Phys. Rev. B **71**, 033303 (2005).
- <sup>23</sup> N. D. Drummond, M. D. Towler, and R. J. Needs, Phys. Rev. B **70**, 235119 (2004).
- <sup>24</sup> P. López Ríos, P. Seth, N. D. Drummond, and R. J. Needs, Phys. Rev. E **86**, 036703 (2012).
- <sup>25</sup> T. Kato, Commun. Pure Appl. Math. **10**, 151 (1957).
- <sup>26</sup> R. T. Pack and W. Byers Brown, J. Chem. Phys. **45**, 556 (1966).
- <sup>27</sup> C. J. Umrigar, K. G. Wilson, and J. W. Wilkins, Phys. Rev. Lett. **60**, 1719 (1988).
- <sup>28</sup> N. D. Drummond and R. J. Needs, Phys. Rev. B **72**, 085124 (2005).
- <sup>29</sup> J. Toulouse and C. J. Umrigar, J. Chem. Phys. **126**, 084102 (2007).
- <sup>30</sup> G. G. Spink, P. López Ríos, N. D. Drummond, and R. J. Needs, Phys. Rev. B **94**, 041410 (2016).
- <sup>31</sup> D. M. Ceperley and M. H. Kalos, in *Monte Carlo methods in statistical physics*, edited by K. Binder (Springer-Verlag, Heidelberg, 1979) 2nd ed., p. 145.
- <sup>32</sup> The top-left element of the matrix  $f$  in Eq. (13) is the fitting parameter  $f_{00}$ , and so on.